



HAL
open science

CONTROL PARAMETERS FOR REED WIND INSTRUMENTS OR ORGAN PIPES WITH REED INDUCED FLOW

Juliette Chabassier, Roman Auvray

► **To cite this version:**

Juliette Chabassier, Roman Auvray. CONTROL PARAMETERS FOR REED WIND INSTRUMENTS OR ORGAN PIPES WITH REED INDUCED FLOW. DAFx 20in22, Sep 2022, Vienna, Austria. hal-03794382

HAL Id: hal-03794382

<https://hal.science/hal-03794382v1>

Submitted on 3 Oct 2022

HAL is a multi-disciplinary open access archive for the deposit and dissemination of scientific research documents, whether they are published or not. The documents may come from teaching and research institutions in France or abroad, or from public or private research centers.

L'archive ouverte pluridisciplinaire **HAL**, est destinée au dépôt et à la diffusion de documents scientifiques de niveau recherche, publiés ou non, émanant des établissements d'enseignement et de recherche français ou étrangers, des laboratoires publics ou privés.

CONTROL PARAMETERS FOR REED WIND INSTRUMENTS OR ORGAN PIPES WITH REED INDUCED FLOW

Juliette Chabassier and Roman Auvray

Modartt

Bât B18, 9 Avenue de l'Europe, Ramonville, France

chabassier@modartt.com | auvray@modartt.com

ABSTRACT

Sound synthesis of a pipe coupled with a reed requires to finely tune the physical parameters of the underlying model. Although the pipe geometry is often well known, the 1 degree of freedom reed model's parameters are effective coefficients (mass, section, etc) and are difficult to assess. Studies of this coupled system have essentially focused on models without the reed induced flow, and have exhibited two dimensionless parameters γ and ζ , which respectively describe the ratio between feeding pressure and closing reed pressure, and a dimensionless opening of the reed at rest. Including the reed flow in the model, then performing a scaling of the equations, leads to a new third dimensionless quantity that we will call κ . Varying the reed frequency with constant (γ, ζ, κ) on different pipe dimensions shows a certain stability of the model once put under this form. Using a real-time sound synthesis tool, the parameter space (γ, ζ, κ) is explored while the damping of the reed is also varied.

1. MODEL

Modeling reed instruments [1, 2] can be done by coupling a linear pipe described with an impedance with a lumped oscillator describing the evolution of the reed opening y in m and satisfying the following equations

$$d_t^2 y + g d_t y + \omega_0^2 (y - y_0) = -\frac{S_r}{M_r} \Delta p \quad (1)$$

$$p(0) = p_m - \Delta p \quad (2)$$

$$\lambda + w y^+ \sqrt{\frac{2|\Delta p|}{\rho}} \text{sign}(\Delta p) - S_r d_t y = 0 \quad (3)$$

$$\frac{\hat{p}(0)}{\hat{\lambda}} = Z_{in} Z(\omega), \quad (4)$$

where the characteristic input impedance is

$$Z_{in} = \frac{\rho c}{S_{in}} \quad (5)$$

with ρ and c the density and celerity of air, S_{in} the input section of the pipe, and where the physical or effective parameters are referred to as ω_0 and f_0 the reed pulsation and frequency in Hz, S_r the reed section in m^2 , M_r the reed mass in kg, y_0 the reed opening at rest in m, g the reed damping in s^{-1} , w the reed width in

m and p_m the feeding pressure in Pa. Attempts to quantify their precise values have been done in many directions, as direct measurements on the reed [3, 1], geometrical equivalence to the first vibration mode of a beam [4, 5], and inverse estimation [2, 6, 7]. Acoustic variables at the pipe entry are the pressure $p(0)$ and the acoustic flow λ . While the pipe equations can be described in the harmonic domain, due to nonlinear effects, the reed equations must be considered in the time domain. Note that the reed induced flow is modelled here by the $S_r d_t y$ term in Eq. 3. This term can be considered as equivalent to adding a compliance in parallel to the pipe input impedance linked to an effective length correction ΔL [8, 9, 10].

2. SCALING

Searching for static solutions to Eq. (1) naturally prompts a closing pressure

$$P_{plac} = \frac{M_r}{S_r} y_0 \omega_0^2 \quad (6)$$

Multiplying Eq. (1) with $\frac{1}{y_0}$, Eq. (2) with $\frac{1}{P_{plac}}$, and Eq. (3) with $\frac{Z_{in}}{P_{plac}}$, one gets

$$d_t^2 \frac{y}{y_0} + g d_t \frac{y}{y_0} + \omega_0^2 \left(\frac{y}{y_0} - 1 \right) = -\omega_0^2 \frac{\Delta p}{P_{plac}} \quad (7)$$

$$\frac{p(0)}{P_{plac}} = \frac{p_m}{P_{plac}} - \frac{\Delta p}{P_{plac}} \quad (8)$$

$$Z_{in} \frac{\lambda}{P_{plac}} + \sqrt{\frac{2}{\rho P_{plac}}} Z_{in} w y_0 \frac{y^+}{y_0} \sqrt{\frac{|\Delta p|}{P_{plac}}} \text{sign}(\Delta p) - \frac{Z_{in} S_r}{P_{plac}} y_0 d_t \frac{y}{y_0} = 0 \quad (9)$$

$$\frac{\hat{p}(0)}{P_{plac}} = \frac{Z_{in} \hat{\lambda}}{P_{plac}} Z(\omega), \quad (10)$$

This procedure lets naturally appear [11, 12, 1, 13, 14] the two dimensionless parameters γ and ζ :

$$\gamma = \frac{p_m}{P_{plac}}, \quad \zeta = Z_{in} w y_0 \sqrt{\frac{2}{\rho P_{plac}}} \quad (11)$$

However, the term in Eq. (9) driving $d_t \frac{y}{y_0}$ is not dimensionless, it is homogeneous to a time. It is therefore natural to introduce κ as

$$\kappa = \frac{Z_{in} S_r y_0}{P_{plac}} \omega_0 = \frac{Z_{in} S_r^2}{M_r \omega_0} \quad (12)$$

Copyright: © 2022 Juliette Chabassier et al. This is an open-access article distributed under the terms of the Creative Commons Attribution 4.0 International License, which permits unrestricted use, distribution, adaptation, and reproduction in any medium, provided the original author and source are credited.

A scaling of the unknowns is then proposed following [15] as

$$y \rightarrow y_0 y, \quad \lambda \rightarrow P_{plac} \frac{\lambda}{Z_{in}}, \quad p \rightarrow P_{plac} p, \quad (13)$$

and the reed quality factor Q_r is introduced as

$$Q_r = \frac{\omega_0}{g} \quad (14)$$

so that the scaled equations now read

$$\frac{1}{\omega_0^2} d_t^2 y + \frac{1}{Q_r \omega_0} d_t y + y = 1 - \Delta p \quad (15)$$

$$p(0) = \gamma - \Delta p \quad (16)$$

$$\lambda + \zeta y^+ \sqrt{|\Delta p| \text{sign}(\Delta p)} - \frac{\kappa}{\omega_0} d_t y = 0 \quad (17)$$

$$\hat{p}(0) = \hat{\lambda} Z(\omega) \quad (18)$$

The collection of 7 physical parameters and the knowledge of the pipe geometry are now reduced to a collection of 5 meta-parameters ($\gamma, \zeta, \kappa, Q_r, \omega_0$) and the knowledge of the pipe geometry that control the equations without any simplification, meaning that the obtained system is mathematically equivalent to the original one, e.g. the same set of solutions can be achieved. It implies that, in the original system, the same solution ($y, \lambda, p(0)$) can be obtained from several choices of dimensioned parameters that lead to the same meta-parameters. Note that

$$\kappa = \frac{\Delta L}{c} \omega_0 \quad (19)$$

where $\Delta L = Z_{in} S_r y_0 c / P_{plac}$ following [8, 9, 10].

3. LINK BETWEEN DIMENSIONED AND META PARAMETERS

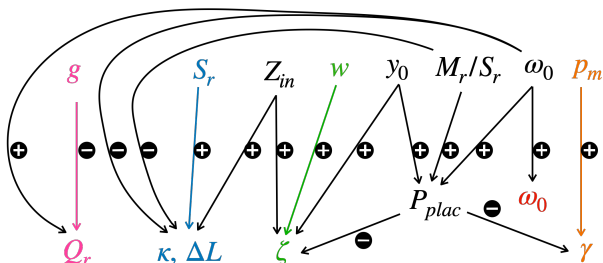


Figure 1: Link between dimensioned and meta parameters. A plus sign means that increasing the dimensioned parameter will increase the scaled one, a minus sign means that increasing the dimensioned parameter will decrease the scaled one.

Values for dimensioned parameters are available in the literature [4, 3, 1, 2, 7, 5] and allow to compute the scaled parameters using Eqs. (11) for γ and ζ , Eq. (12) for κ , where P_{plac} is defined in Eq. (6). This procedure is summed up in Tab. 1, where parameters in *italic* are guessed because their value could not be found in the reference. Values above (resp. below) the double line concern clarinet-like (resp. organ-like) instruments. Fig. 1 illustrates a possible view of the dependancy between the dimensioned and meta parameters. The dimensioned parameters have been considered as ($g, S_r, Z_{in}, w, y_0, M_r/S_r, \omega_0, p_m$). Notice that M_r is

not considered as an independent parameter but rather in the ratio M_r/S_r , because this choice limits the number of dependencies. Fig. 1 highlights the fact that some of those dimensioned parameters can be considered as principal drivers of the meta parameters, since they do not appear in the definition of the other meta parameters. It is the case of p_m which drives only γ , w which drives only ζ , S_r which drives only κ and g which drives only Q_r . An interesting observation is that the dimensioned ω_0 does not contribute only to the ω_0 appearing in the scaled equations, but also to P_{plac} and therefore, indirectly, to γ and ζ .

The first question that arises is then : is the model easier to tune when it is driven with dimensioned parameters or with scaled parameters ? The simple fact that the new system is mathematically equivalent to the original one, with only 5 control parameters instead of 8 (the 7 previous ones augmented with the input impedance of the pipe), points towards the scaled framework. Moreover, Tab. 1 shows that from the values of dimensioned parameters found in the literature and leading to oscillating solutions, the scaled parameters are always of the order of 1, which makes them easier to infer than the dimensioned ones. This is also observed on meta parameters used in the literature, as illustrated in Tab. 2.

And a second question follows : how are the parameters supposed to be related ? In the context of physical modelling aiming at simulation/experiment comparison, the parameters are expected to reflect a certain reality, obtained from direct geometrical measurements on the reed [3, 1], model reduction [4, 5], or inverse estimation of parameters from experimental calibration [2, 6, 7]. Therefore, the parameters of the model reflect a physical configuration and are not really independent (the mass, section, width and vibrating frequency follow from the laws of a vibrating beam, for instance). Following [16], dimensioned parameters can be expressed as functions of the lateral and vibrating lengths of the reed. Modeling the behaviour of a reed organ pipe during tuning is therefore possible by imposing those relations and modifying the dimensioned parameters accordingly. A possible interpretation of these relations leads to Fig. 2, where it can be observed that the sounding frequency increases as the reed length decreases on a pipe of a trumpet rank of the Cavaillé-Coll organ located in Royaumont (France)[17]. This figure is very similar to Fig. 7 of [16], illustrating the capacity of this simple model to account for organ pipes behaviours, which motivates its use in a synthesis context. Indeed, the present work focuses on real time physically informed sound synthesis, but targets sound realism rather than quantitative match with experimental data. In this context, the motivation is not to tune the model parameters to values that reflect an experimental apparatus, but to find parameter values that produce a realistic sound. The angle chosen here is therefore to explore the parameters space in the most predictable way possible, so to obtain the expected sounds from a given instrument. This is one supplementary reason why the use of meta parameters, by reducing the dimension of the parameter space, seems a good direction.

4. SYNTHESIS

The behaviour of the scaled model is investigated by making the meta-parameters vary, and performing a sound synthesis with the real time engine Organteq [20]. The impedance of the pipe is de-

Table 1: Computed meta parameters from dimensioned values found in the literature. Parameters in *italic* are guessed because their value could not be found in the reference. Values above (resp. below) the double line concern clarinet-like (resp. organ-like) instruments.

	M_r/S_r (kg/m ²)	S_r (m ²)	y_0 (m)	w (m)	Z_{in}	p_m (Pa)	g (s ⁻¹)	$\omega_0/(2\pi)$ (Hz)	P_{plac} (Pa)	γ w.d.	ζ w.d.	κ w.d.	Q_r w.d.
[4] - Fig 10.17 A*	5.20e-2	8.00e-5	8.50e-4	1.00e-2	2.85e6	2000	3000	1900	6.30e3	0.32	0.38	0.37	4.0
[4] - Fig 10.17 B*	3.50e-2	5.50e-5	1.06e-3	1.00e-2	2.85e6	2000	3000	2400	8.44e3	0.24	0.41	0.30	5.0
[4] - Fig 10.17 C*	3.50e-2	3.80e-5	1.23e-3	1.00e-2	2.85e6	2000	30000	3000	1.53e4	0.13	0.35	0.16	0.6
[3] - Tab. I	2.31e-2	1.46e-4	4.00e-4	6.34e-2	2.29e6	2265	3000	3700	4.99e3	0.45	1.02	0.62	7.8
[1] - Fig. 7	2.31e-2	1.46e-4	4.00e-4	1.00e-2	2.55e6	3000	3000	3700	4.99e3	0.60	0.18	0.69	7.7
[2] - Tab. I	5.00e-2	7.00e-5	4.00e-4	1.30e-2	4.62e6	1800	3000	2747	5.96e3	0.30	0.39	0.37	5.8
[2] - Tab. II	5.60e-2	1.77e-4	2.55e-4	1.20e-2	4.62e6	1800	453	2368	3.16e3	0.57	0.31	0.98	32.8
[6] - Tab VI	2.69e-1	1.00e-4	3.60e-4	1.00e-2	2.85e6	1000	3717	672	1.73e3	0.58	0.31	0.25	1.1
[7] - initial	3.30e-2	9.86e-5	2.46e-4	1.20e-2	2.85e6	4500	3000	3709	4.40e3	1.02	0.16	0.37	7.8
[5]	2.63	2.16e-4	3.60e-4	3.72e-2	6.60e6	800	99	220	1.81e3	0.44	2.59	0.39	14.0

* The three lines A,B and C are three chosen values in Fig. 10.16 and 10.17 of [4], corresponding to the indicated values of y_0 .

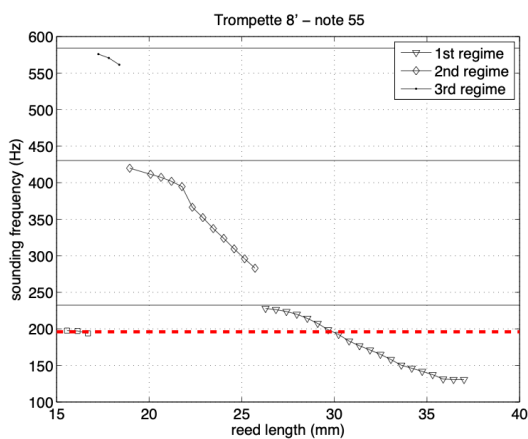


Figure 2: Sounding frequency of the system with respect to the reed vibrating length. The pipe is composed of two cones of lengths 67.2mm and 639.3mm (total 706.6mm), with radii (from bottom to top) 3.3mm, 1.7mm, 19.2mm. Its three first resonances frequencies are indicated as horizontal solid lines at 232.39 Hz, 430.43Hz and 584.20Hz. The reed quality factor is set to $Q_r = 100$.

Table 2: Values of meta parameters found in the literature. Values above (resp. below) the double line concern clarinet-like (resp. organ-like) instruments.

	$\omega_0/(2\pi)$ (Hz)	γ w.d.	ζ w.d.	κ w.d.	Q_r w.d.
[18] - Fig. 14	2205	.4	.4	0	3.3
[18] - Fig. 15	1850	$\approx .4$	$\approx .2$	0	5
[12] - Fig. 1	750	≈ 0.5	0.13	0	2.5
[19] - Fig 7 R1**	?	0.4	0.495	?	?
[19] - Fig 7 R2**	?	0.35	0.26	?	?
[19] - Fig 7 R3**	?	0.45	0.34	?	?
[19] - Fig 7 QP**	?	0.35	0.36	?	?
[12] - Fig. 2	700	≈ 0.25	0.10	0	125

** The four lines R1, R2, R3 and QP are four chosen values in Fig. 7 of [19] for which the regimes seem stable as the pipe inharmonicity varies.

scribed under the form

$$Z(\omega) = \sum_{Im(\mu_k)=0} \frac{c_k}{j\omega + d_k} + \sum_{Im(\mu_k)>0} \left[\frac{Z_c C_k^{BP}}{1 + jQ_k \left(\frac{\omega}{\omega_k} - \frac{\omega_k}{\omega} \right)} + \frac{Z_c C_k^{LP}}{1 + jQ_k^{-1} \frac{\omega}{\omega_k} + \left(\frac{\omega}{\omega_k} \right)^2} \right]$$

where the modal coefficients (complex eigenvalue μ_k with imaginary part $\omega_k = 2\pi f_k$ and real part $d_k = -\omega_k/(2Q_k)$) being related to the eigenfrequency f_k and quality factor Q_k of each pipe mode), are computed by solving a generalized eigenvalue problem based on the pipe geometry. As presented in [21], this method accounts for the pipe section variations, radiation at the bell, viscothermal effects near the boundary (thermo-viscous losses), possibly chimneys and radiation at the chimneys top. The modal coefficients obtained with this method preserve the well-posed character of the equations even after modal truncation, and ad-hoc time integrators have been derived to perform real time simulations.

The following examples are performed on pipes

- P1: a cylinder of length $L = 0.5$ m and radius $R = 0.01$ m.
- P2: a cone of length $L = .5$ m, input radius $R = 0.005$ m and output radius $R = 0.03$ m.

- P3: a ‘‘Vox Humana’’ pipe half-closed at the pipe end, with dimensions

x (mm)	0	60.6	60.6	99.6	189.3
R (mm)	3	3	6	14.4	14.4

The analysed output of the system is the time derivative of the acoustic flow at the bell.

5. SOUNDING FREQUENCY

In this section we study the sounding frequency of the three considered pipes with respect to the reed frequency obtained for

$$Q_r \in \{2.5, 125\} \quad (20)$$

$$\kappa \in \{10^{-3}, 0.1, 0.5, 0.8\} \quad (21)$$

$$\gamma = 0.5 \quad (22)$$

$$\zeta = 0.8 \quad (23)$$

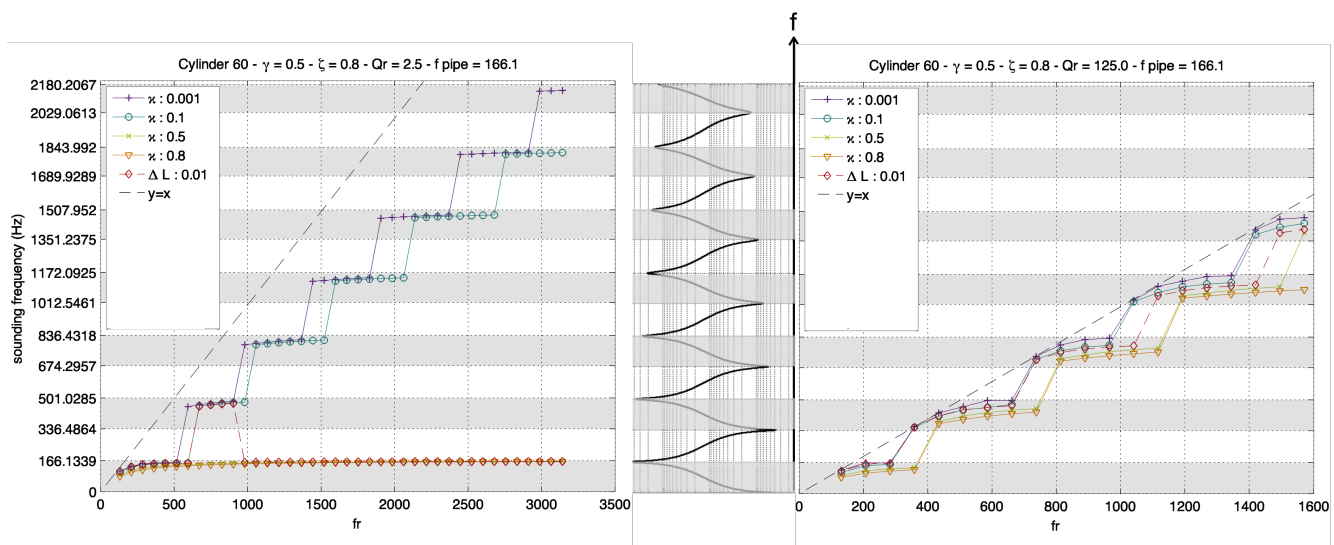


Figure 3: Sounding frequency w.r.t. reed frequency, pipe P1, for different values of $\kappa \in \{10^{-3}, 0.1, 0.5, 0.8\}$ and for $\Delta L = 0.01$. Left: strongly damped reed. Right: slightly damped reed. Pipe impedance magnitude in log scale in the middle.

Fig. 3 displays the sounding frequency of pipe P1 with respect to the reed frequency in different colours corresponding to several values of κ . Two values of Q_r are considered: 2.5 corresponds to a strongly damped reed (typically made of cane) while 125 corresponds to a slightly damped reed (typically made of metal). The sounding frequency always increases with the reed frequency, although not uniformly. Changes of regime can indeed be observed for both values. The instrument always sounds in the gray bands, which correspond to increasing parts of the impedance magnitude. At a given reed frequency, smaller values of κ lead to higher pitched sounds. For the strongly damped reed ($Q_r = 2.5$, typical of cane reeds), high values of κ induce a “clarinet-like” behaviour: the heard note is driven by the pipe and not by the reed frequency. In all other cases (strongly damped reed with high values of κ , and slightly damped reed with any value of κ), the heard note follows a regime change as the reed frequency increases, inducing an “organ-like” behaviour. Finally, following the curve labelled $\Delta L = 0.01$ means that κ is adjusted for each reed frequency in order to fit a prescribed value for ΔL (see Eq (19)). This leads to a more erratic behaviour of the instrument, which shows that using dimensionless parameters could help tuning sound synthesis.

Fig. 4 and Fig. 5 display the same data obtained for pipes P2 and P3. Almost the same conclusions can be drawn except that the sounding frequency sometimes does not increase with the reed frequency. This is due to multi-phonic sounds that can appear: either a first (high) frequency is heard and then the system chooses another (lower) frequency to stabilise on, or both frequencies can be heard at the same time. Sounds will be heard during the presentation to illustrate those phenomena.

6. CARTOGRAPHY

In this section we display a multi-cartography obtained for pipe P1 and

$$\omega_r = 2\pi \times 170 \quad (24)$$

$$Q_r \in \{2.5, 20, 60, 125\} \quad (25)$$

$$\kappa \in \{10^{-3}, 10^{-2}, 0.1, 0.5, 0.8\} \quad (26)$$

$$\gamma \in \{0.1, 0.2, 0.3, 0.4, 0.5, 0.6, 0.7, 0.8, 0.9, 1\} \quad (27)$$

$$\zeta \in \{0.2, 0.4, 0.6, 0.8, 1, 1.2, 1.4, 1.6, 1.8, 2\} \quad (28)$$

Fig. 6 and Fig. 7 display unitary cartographies in the plane (γ, ζ) , organised in the larger plane (Q_r, κ) . Fig. 6 shows the deviation between the playing frequency ω and the reed frequency ω_0 , in cents:

$$d = 1200 \times \log_2\left(\frac{\omega}{\omega_0}\right) \quad (29)$$

Color scale is the same for all figures, ranging from 0 (red) to -1200 cents (blue). In the considered values range, larger values of κ lead to more stable behaviours, consistently with the result displayed in Fig. 3. Depending on the regime, increasing γ can sometimes lead to lowering the pitch. Fig. 7 shows the spectral centroid defined as the relative gravity center of the harmonics of the signal. Color scale is the same for all figures, ranging from 0 to 9. In general, the sound seems to get brighter as Q_r gets higher (slightly damped reed) and as κ gets small. Careful analysis of the different figures shows that increasing γ tends to increase the spectral centroid, while ζ influences the brightness of the sound in a non trivial way.

7. CONCLUSIONS

Using the scaled version of the reed equations controlled with 5 meta-parameters $(\gamma, \zeta, \kappa, Q_r, \omega_0)$ is a practical way of exploring the parameters range in the context of sound synthesis as done in

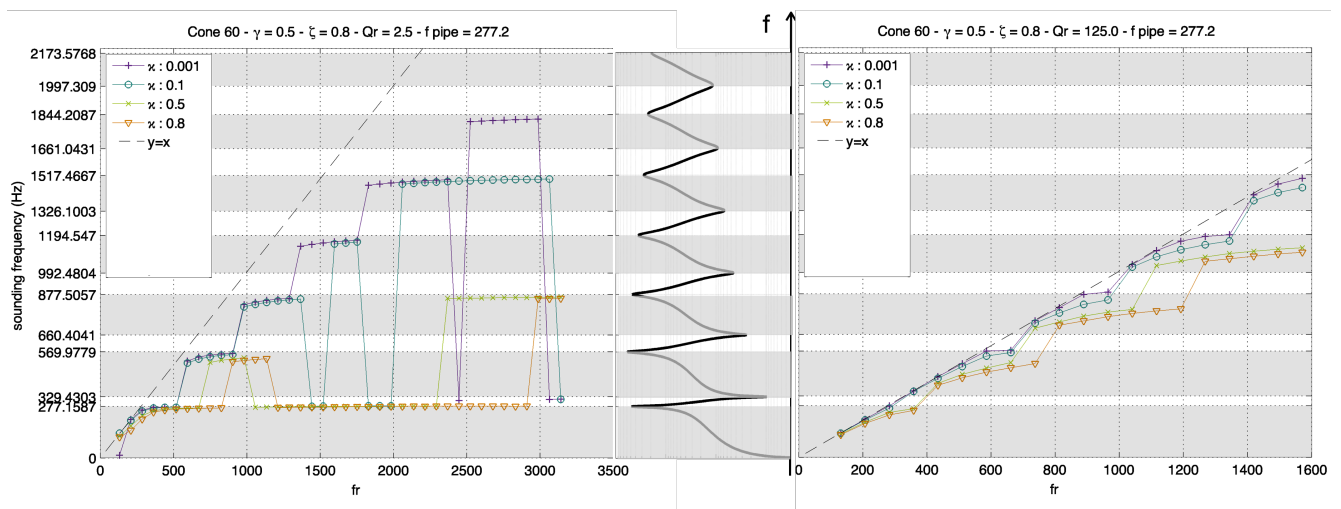


Figure 4: Sounding frequency w.r.t. reed frequency, pipe P2, for different values of $\kappa \in \{10^{-3}, 0.1, 0.5, 0.8\}$. Left: strongly damped reed. Right: slightly damped reed. Pipe impedance magnitude in log scale in the middle.

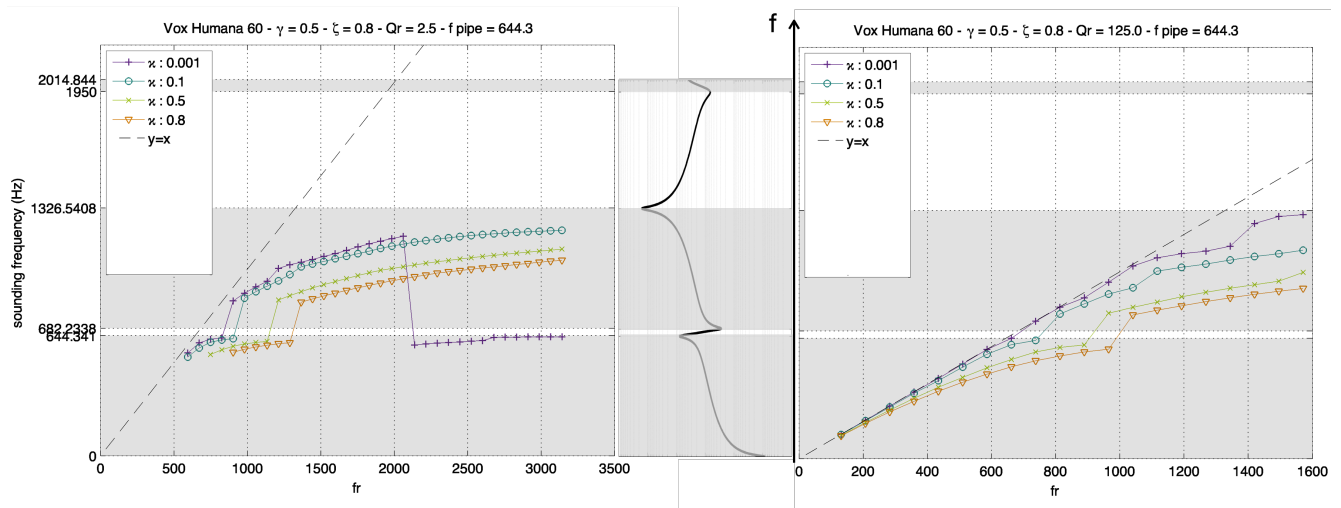


Figure 5: Sounding frequency w.r.t. reed frequency, pipe P3, for different values of $\kappa \in \{10^{-3}, 0.1, 0.5, 0.8\}$. Left: strongly damped reed. Right: slightly damped reed. Pipe impedance magnitude in log scale in the middle.

the commercial software Organteq. This allows to perform systematic cartographies of a pipe’s behaviour, leading to more stable results than using dimensioned parameters. Although γ and ζ were known in the literature, to the best of our knowledge, our formula for κ is new and seems to constitute an interesting viewpoint on the model by completing the scaling with dimensionless parameters. In the presentation, sounds will be heard to illustrate the presented curves. Open questions arise, as how variations of physical parameters during playing [2, 6, 7] will impact in the meta-parameters.

8. REFERENCES

- [1] Stefan Bilbao, “Direct simulation for wind instrument synthesis,” in *Conference on Digital Audio Effects*. Citeseer, 2008, pp. 145–152.
- [2] Vasileios Chatzioannou and Maarten van Walstijn, “Estimation of clarinet reed parameters by inverse modelling,” *Acta Acustica united with Acustica*, vol. 98, no. 4, pp. 629–639, 2012.
- [3] Federico Avanzini and Davide Rocchesso, “Efficiency, accuracy, and stability issues in discrete-time simulations of single reed wind instruments,” *The Journal of the Acoustical Society of America*, vol. 111, no. 5, pp. 2293–2301, 2002.
- [4] Maarten Van Walstijn, *Discrete-time modelling of brass and reed woodwind instruments with application to musical sound synthesis*, Ph.D. thesis, 01 2002.
- [5] András Miklós, Judit Angster, Stephan Pitsch, and Thomas D Rossing, “Reed vibration in lingual organ pipes without the resonators,” *The Journal of the Acoustical Society of America*, vol. 113, no. 2, pp. 1081–1091, 2003.

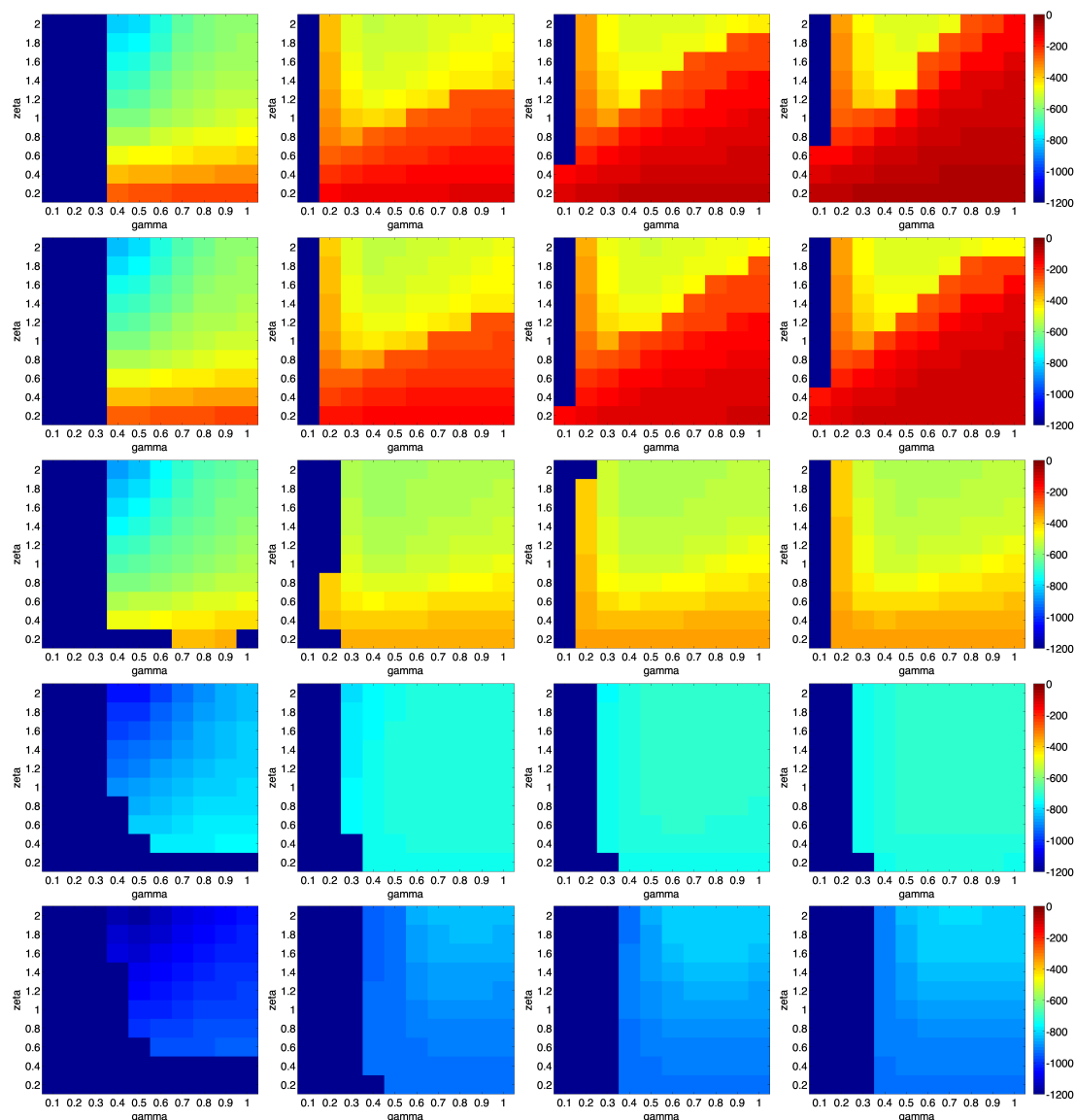


Figure 6: Deviation between the playing frequency and the reed frequency, in cents. Color scale is the same for all figures, ranging from 0 (red) to -1200 cents (blue). From left to right: $Q_r \in \{2.5, 20, 60, 125\}$. From top to bottom: $\kappa \in \{10^{-3}, 10^{-2}, 0.1, 0.5, 0.8\}$

[6] Alberto Muñoz Aracón, Bruno Gazengel, Jean-Pierre Dalmont, and Ewen Conan, “Estimation of saxophone reed parameters during playing,” *J. Acous. Soc. Am.*, vol. 139, no. 5, pp. 2754–2765, 2016.

[7] Vasileios Chatziioannou, Sebastian Schmutzhard, Montserrat Pàmies-Vilà, and Alex Hofmann, “Investigating clarinet articulation using a physical model and an artificial blowing machine,” *Acta Acustica United with Acustica*, vol. 105, no. 4, pp. 682–694, 2019.

[8] Cornelis Johannes Nederveen, *Acoustical aspects of woodwind instruments*, Frits Knuf, 1969.

[9] Jean-Pierre Dalmont, Bruno Gazengel, Joël Gilbert, and Jean Kergomard, “Some aspects of tuning and clean intonation in reed instruments,” *Applied acoustics*, vol. 46, no. 1, pp. 19–60, 1995.

[10] Antoine Chaigne and Jean Kergomard, *Acoustics of musical instruments*, Springer, 2016.

[11] Theodore A Wilson and Gordon S Beavers, “Operating modes of the clarinet,” *J. Acous. Soc. Am.*, vol. 56, no. 2, pp. 653–658, 1974.

[12] Fabrice Silva, Jean Kergomard, Christophe Vergez, and Joël Gilbert, “Interaction of reed and acoustic resonator in clarinetlike systems,” *J. Acous. Soc. Am.*, vol. 124, no. 5, pp. 3284–3295, 2008.

[13] Sami Karkar, Christophe Vergez, and Bruno Cochelin, “Oscillation threshold of a clarinet model: A numerical contin-

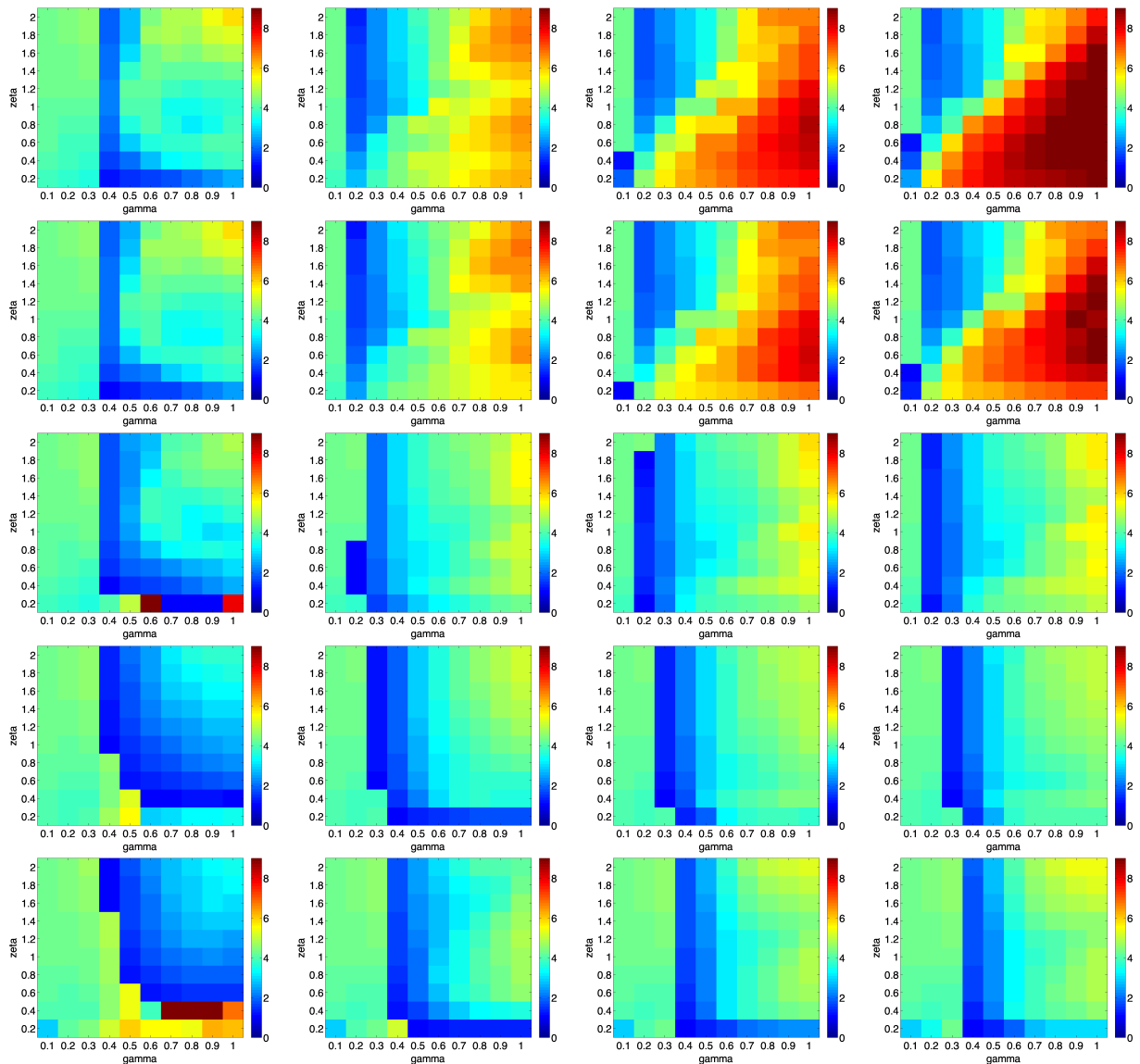


Figure 7: Relative spectral centroid. From left to right: $Q_r \in \{2.5, 20, 60, 125\}$. From top to bottom: $\kappa \in \{10^{-3}, 10^{-2}, 0.1, 0.5, 0.8\}$

uation approach,” *J. Acous. Soc. Am.*, vol. 131, no. 1, pp. 698–707, 2012.

[14] T Colinot, *Numerical simulation of woodwind dynamics: investigating nonlinear sound production behavior in saxophone-like instruments*, Ph.D. thesis, Aix-Marseille Université (AMU), 2020.

[15] A Hirschberg, *Mechanics of Musical Instruments (Chap. 6, J. Kergomard)*, chapter Elementary considerations on reed-instrument oscillations, 1995.

[16] András Miklós, Judit Angster, Stephan Pitsch, and Thomas D Rossing, “Interaction of reed and resonator by sound generation in a reed organ pipe,” *The Journal of the Acoustical Society of America*, vol. 119, no. 5, pp. 3121–3129, 2006.

[17] “Plet laurent, website,” <http://lplet.org>, Accessed: 2022-06-12.

[18] Philippe Guillemain, Jean Kergomard, and Thierry Voinier, “Real-time synthesis of clarinet-like instruments using digital impedance models,” *The Journal of the Acoustical Society of America*, vol. 118, no. 1, pp. 483–494, 2005.

[19] J-B Doc and Christophe Vergez, “Analyse expérimentale de l’effet de l’inharmonicité des instruments a anche simple-cas du saxophone alto,” in *12ème Congrès Français d’Acoustique de Poitiers*, 2014.

[20] “organteq website,” <http://organteq.com>, Accessed: 2022-06-12.

[21] Juliette Chabassier and Roman Auvray, “Direct computation of modal parameters for musical wind instruments,” *Journal of Sound and Vibration*, vol. 528, pp. 116775, 2022.